Available online at www.sciencedirect.com
ScienceDirect
Ceramics International 35 (2009) 345–347
CERAMICS INTERNATIONAL
www.elsevier.com/locate/ceramint

Magnetic and magnetoresistive properties of $La_{0.65-x}Eu_xSr_{0.35}MnO_3$

Ming Feng [a], Hai-bo Li [a,*], Mei Liu [a], Na Li [a], Wei-tao Zheng [b]

[a] *Institute of Condensed Matter Physics and Materials Science, Jilin Normal University, Siping 136000, PR China*
[b] *Department of Materials Science, Jilin University, Changchun 130012, PR China*

Received 3 September 2007; received in revised form 8 September 2007; accepted 3 November 2007
Available online 10 January 2008

Abstract

Eu-doped perovskites $La_{0.65-x}Eu_xSr_{0.35}MnO_3$ ($0.05 \leq x \leq 0.30$) were synthesized by sol–gel method using citric acid and characterized by X-ray diffraction, magnetization, resistivity and magnetoresistance (MR) experiments. All samples had a single hexagonal perovskite structure. As x increased from 0.05 to 0.30, the Curie temperature T_C for the samples decreased from 352 to 242 K. It was found that two transition points appeared when the resistivity changed with increasing temperature, and upon an application of a magnetic field of 20 kOe the maximum magnetoresistivity of 18% for the $La_{0.65-x}Eu_xSr_{0.35}MnO_3$ with $x = 0.20$ was obtained at room temperature 300 K. The mechanism of the transitions for the samples was explored.

Keywords: A. Sol–gel processes; B. X-ray methods; C. Electrical properties; C. Magnetic properties; D. Perovskites

1. Introduction

Over the past few years, perovskite manganites $A_{1-x}A'_xMnO_3$ (A = trivalent rare earth; A′ = divalent alkaline earth metal or monovalent alkali metal) have received special attention due to many fascinating properties such as insulator–metal transition (I–M), colossal magnetoresistance (CMR), magnetocaloric effect (MCE) and charge, orbital, spin ordering [1–3]. Undoped $LaMnO_3$ is antiferromagnetic insulator, and substitution of divalent ions for La^{3+} creates a Mn^{3+}–Mn^{4+} mixed valence state resulting in mobile charge carriers and canting of Mn spins. Then, $LaMnO_3$ can be driven into a metallic and ferromagnetic state. Both Mn^{3+} and Mn^{4+} ions possess a local spin ($S = 3/2$) from their lower t_{2g}^3 orbital, and Mn^{3+} has an extra electron in the e_g orbital which is responsible for conduction. The double exchange (DE) interaction [4] between Mn^{3+} and Mn^{4+} ions, along with the Jahn–Teller distortion, leads to the appearance of the so-called CMR in such systems. Millis et al. argued that the physics of manganites is dominated by the interplay between a strong electron–phonon coupling and the large Hund coupling effects that optimizes the electronic kinetic energy by the formation of ferromagnetic phase [5,6]. However, other factors, namely, average A-site cationic radius, mismatch effects, competition between the ferromagnetic and the charge-ordered phases, vacancies in La- and Mn-sites and the oxygen stoichiometry, also play an important role.

A family of Sr-doped $La_{1-x}Sr_xMnO_3$ manganites has attracted the widest interest in aspects of experimental and theoretical researches, because they exhibit the largest CMR effect [7–9]. However, the Curie temperature (T_C) value of this material family is about 370 K, still far away from room temperature. Fortunately, as the T_C and magnetization of perovskite manganites can be adjusted by either La-site or Mn-site doping, the CMR effect of perovskite manganites can be tuned to near room temperature, which is beneficial for manipulating magnetoresistivity that occurs in various temperature ranges [10]. In this study, we try to lower the metal–semiconductor transition temperature, which is usually nearly coincident with the Curie temperature, nearly to the room temperature so that large MR can be obtained around the room temperature.

2. Experimental

A series of $La_{0.65-x}Eu_xSr_{0.35}MnO_3$ bulk samples were synthesized by sol–gel technique using citric acid (CA). The

* Corresponding author. Tel.: +86 434 3290232; fax: +86 434 3292210.
E-mail address: lihaibo@jlnu.edu.cn (H.-b. Li).

0272-8842/$34.00
doi:10.1016/j.ceramint.2007.11.004

stoichiometric amounts of analytical reagents of $La(NO_3)_3$, Eu_2O_3, $Sr(NO_3)_2$, $Mn(NO_3)_2$ were dissolved in dilute HNO_3 solution. A certain amount of citric acid (molar ration: CA/all the metallic ions = 2) as chelating agents was introduced into the above mixture. The mixture was magnetically stirred for 2 h. Clear and transparent sol was obtained after complete dissolution, which was evaporated on a water bath at 363 K to remove the excess water, and then the gel is formed. The gel was dried at 473 K in baking oven until xerogel formed. The xerogel was slowly heated to 873 K and pre-calcined for 5 h to make the organic matter decompose completely. The obtained powders were ground, pelletized, and calcined at 1473 K for 10 h.

The structure of polycrystalline $La_{0.65-x}Eu_xSr_{0.35}MnO_3$ samples were characterized by X-ray diffraction (XRD) using a D/max-2500/PC system with the Cu Kα radiation and measured at room temperature. High-purity silicon powders were used as an internal standard to determine the lattice parameters, which was determined from X-ray data using JADE 6.5 software. The magnetic measurements were performed by using Lake Shore M-7407 vibrating sample magnetometer (VSM), and resistivity data were obtained by Quantum Design MPMS-XL-5 system with a standard four-probe method.

3. Results and discussion

Fig. 1 shows the X-ray diffraction patterns for $La_{0.65-x}Eu_xSr_{0.35}MnO_3$ samples with $0.05 \leq x \leq 0.30$ at room temperature. All samples have a single hexagonal perovskite structure. The lattice constants for polycrystalline $La_{0.65-x}Eu_xSr_{0.35}MnO_3$ samples are listed in Table 1, and the average A-site ionic radius, the Curie temperature and the coercivity are also given. The lattice parameters a and the unit cell volume decrease with the Eu content, while the lattice parameter c reaches a minimum value at $x = 0.15$ and then increases as $x > 0.15$. Since the radius of La^{3+} is greater than that of Eu^{3+} in the $La_{1-x}Eu_xSrMnO_3$ system, it is reasonable to observe the reducing lattice constants and the average A-site ionic radius $\langle r_A \rangle$ with the increase in the Eu content.

Table 1
Lattice parameters, cell volume, average A-site ionic radius, and Curie temperature for $La_{0.65-x}Eu_xSr_{0.35}MnO_3$ ($0.05 \leq x \leq 0.30$)

Sample	$x = 0.05$	$x = 0.10$	$x = 0.15$	$x = 0.20$	$x = 0.30$
a (Å)	5.501	5.489	5.486	5.468	5.459
c (Å)	13.342	13.341	13.334	13.350	13.358
V (Å^3)	349.6	348.1	347.6	345.7	344.8
$\langle r_A \rangle$ (Å)	1.208	1.205	1.202	1.199	1.193
T_C (K)	352	343	324	305	242

Fig. 2 shows the temperature dependence of the magnetization (M–T curve) in field cooling (FC) process upon an application of a field 500 Oe for the samples sintered at 1473 K. It is found that the transition occurs in a narrow temperature range, which suggests a good homogeneity of the samples. More interestingly, the shape of the M–T curve remains almost unchanged even the Eu content increases, but all the curves have a sharp drop in magnetization near the transition temperature. Also as listed in Table 1, the data of the Curie temperature T_C, defined as a maximum in the ''absolute value'' of dM/dT, show that T_C shifts towards lower temperature with increasing the Eu content, which can be attributed to the increase in the bending of Mn–O–Mn bond angle that causes an enhancement of carrier effective mass or a narrowing of the band width [11,12]. The working temperature of the potential colossal magnetoresistance material can be changed easily by La-site doping, which is beneficial for the future application in various temperature ranges.

Fig. 3 exhibits the resistivity and magnetoresistance [$MR = (\rho_0 - \rho_H)/\rho_0 \times 100$] for $La_{0.45}Eu_{0.2}Sr_{0.35}MnO_3$ as a function of temperature under an applied magnetic field of zero and 20 kOe. It can be seen from Fig. 3 that the ρ_0–T curves show double peaks. Upon an applied magnetic field, the resistivity drops and the two transition peaks shift towards higher temperature. The sample shows the semiconducting-like

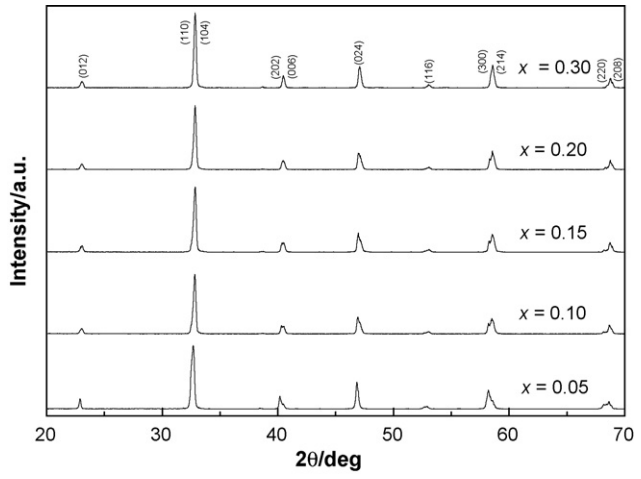

Fig. 1. XRD patterns at room temperature for $La_{0.65-x}Eu_xSr_{0.35}MnO_3$ ($0.05 \leq x \leq 0.30$).

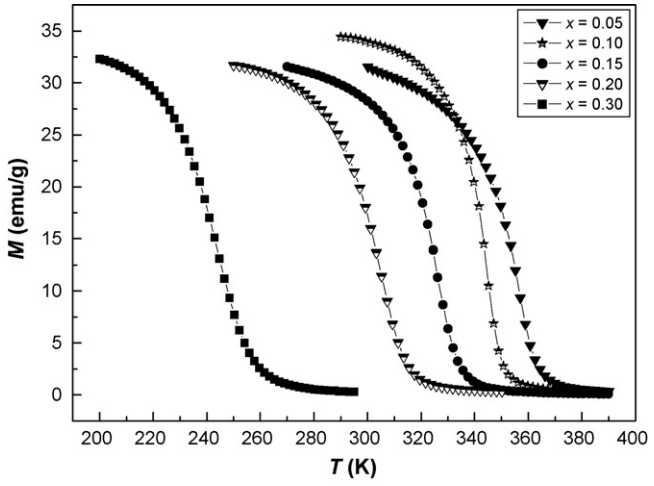

Fig. 2. The temperature dependence of the magnetization in field cooling (FC) process upon an application of a field 500 Oe.

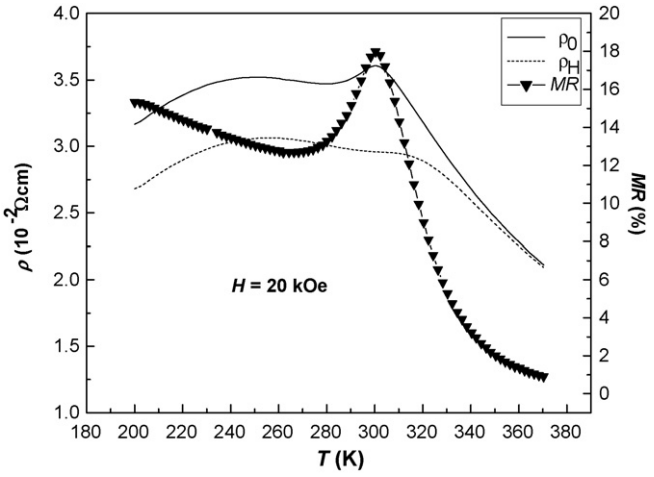

Fig. 3. The resistivity and magnetoresistance as a function of temperature for $La_{0.45}Eu_{0.2}Sr_{0.35}MnO_3$.

and metallic behavior above and below T_C, respectively, similar to that of many other known CMR materials [13,14]. When the temperature drops nearly to the Curie temperature, the thermal disturbance decreases and the lattice scattering also decreases, which makes the scattering relating to the magnetism counterbalance to the lattice scattering. With the drop in temperature, the intensity of the lattice scattering decreases, but the amount of carriers excited also decreases, which leads to the rise in the resistivity. However, when the temperature drops at below the Curie temperature, the spin will transit from disorder to ferromagnetism order. As a result, the scattering intensity relating to the magnetism decreases. Consequently, the e_g electrons become easy to jump between Mn ions, which makes the transfer rate of carriers increase, leading to that the resistivity begin to decrease. Therefore, there appears a metal–semiconductor transition near T_C, which is the direct result that the arrangement of the electronic spin affects the conductive properties when the sample transits from the paramagnetic phase to the ferromagnetism phase. As the temperature decreases further, the amount of the excited carriers decrease, which leads to that the resistivity rises again. Therefore, the second transition, i.e. the metal–semiconductor transition, occurs. Furthermore, this process occurs in the quite wide range of temperature, which has been demonstrated in the Fig. 3 that the peak of the second transition is smooth and wide. The maximum magnetoresistivity of 18% is observed at 300 K for $La_{0.45}Eu_{0.2}Sr_{0.35}MnO_3$. The result is of practical importance, because it shows that the $La_{0.45}Eu_{0.2}Sr_{0.35}MnO_3$ sample is a promising candidate for room temperature applications such as magnetic sensors, magnetoresistive read heads, and magnetic recording material.

4. Conclusions

Eu-doped perovskites $La_{0.65-x}Eu_xSr_{0.35}MnO_3$ ($0.05 \leq x \leq 0.30$) have been synthesized by sol–gel method using citric acid, which structures have been revealed to have a single hexagonal perovskite structure with a space group R-3c. As the Eu content increases, the T_C will shift towards lower temperature. It has been found that there are two transitions when temperature varies, and the maximum magnetoresistivity of 18% for the sample with $x = 0.20$ in a magnetic field of 20 kOe is obtained 300 K, which makes it possible that the application can be realized at room temperature. The mechanism of the transitions occurred for $La_{0.65-x}Eu_xSr_{0.35}MnO_3$ can be explained by the factors such as lattice scattering, magnetic scattering, the amount of excited carriers, etc.

Acknowledgement

We acknowledge the financial support from the Jilin province government, PR China.

References

[1] R. Mathieu, D. Akahoshi, A. Asamitsu, Y. Tomioka, Y. Tokura, Phys. Rev. Lett. 93 (2004) 227202.
[2] K.F. Wang, F. Yuan, S. Dong, D. Li, Z.D. Zhang, Z.F. Ren, J.-M. Liu, Appl. Phys. Lett. 89 (2006) 222505.
[3] J.S. Amaral, M.S. Reis, V.S. Amaral, T.M. Mendonca, J. Magn. Magn. Mater. 290 (2005) 686–689.
[4] C. Zener, Phys. Rev. B 82 (1951) 403.
[5] A.J. Millis, P.B. Littlewood, B.I. Shraiman, Phys. Rev. Lett. 74 (1995) 5144–5147.
[6] A.J. Millis, I. Boris, R. Shraiman, Mueller, Phys. Rev. Lett. 77 (1996) 175–178.
[7] J.W. Feng, C. Ye, L.P. Hwang, Phys. Rev. B 61 (2000) 12271–12276.
[8] B. Ghosh, S. Kar, L.K. Brar, A.K. Raychaudhuri, J. Appl. Phys. 98 (2005) 094302.
[9] S. Mukhopadhyay, I. Das, Appl. Phys. Lett. 88 (2006) 032506.
[10] K. Cherif, S. Zemni, Ja. Dhahri, M. Oumezzine, M. Ghedira, H. Vincent, J. Alloys Compd. 396 (2005) 29–33.
[11] J. Fontcuberta, B. Martinez, A. Seffar, S. Pinol, J.L. Garcia-Munoz, X. Obradors, Phys. Rev. Lett. 76 (1996) 1122–1125.
[12] S.L. Huang, X.G. Cui, D.H. Wang, Z.D. Han, Y.W. Du, J. Alloys Compd. 398 (2005) 184–187.
[13] M.S. Kim, J.B. Yang, Q. Cai, X.D. Zhou, W.J. James, W.B. Yelon, P.E. Parris, D. Buddhikot, S.K. Malik, Phys. Rev. B 71 (2005) 014433.
[14] O. Chmaissem, B. Dabrowski, S. Kolesnik, J. Mais, J.D. Jorgensen, S. Short, C.E. Botez, P.W. Stephens, Phys. Rev. B 72 (2005) 104426.